Journal of Electrical Engineering 7 (2019) 39-50
doi: 10.17265/2328-2223/2019.02.001

Detecting Deterioration Stages in Epoxy Resins Specimens under Partial Discharge Process

Cristian R. Bonini[1], Marcos U. Maillot[1] and Franco M. Pessana[2]

1. Electrical Engineering Department, General Pacheco Regional Faculty, National Technological University, 288 Hipólito Yrigoyen Avenue, General Pacheco 1617, Argentina

2. Electronic Department, Buenos Aires Regional Faculty, National Technological University, 951 Medrano Street, Buenos Aires 1179, Argentina

Abstract: This paper presents a novel analysis tool based on partial discharge (PD) pulses waveform to determinate deterioration process as the fault evolves carbonizing the insulating medium in epoxy resin specimens. The PD pulses were acquired in the laboratory under controlled conditions; specially designed specimens were tested with a tip-flat electrode configuration immersed in a thermostable polymer (epoxy resin). Then, in the processing step, all acquired PD pulses were characterized with the Shannon entropy, and its variations along the deterioration process were studied. It was observed that the dispersion of this quantity increases with the deterioration of the medium, which allowed identifying different deterioration stages. The evolution of the deterioration has a correlation with the appearance of a greater number of pulses, whose entropy values diverge from average value (close to 2). These new pulses were analyzed using signal processing tools. It was found that there are important differences in the spectral content of each family, in the time-scale characteristics and in the energy distribution of the same frequency bands corresponding to each pulses family. In this work, the deterioration of epoxy resin specimens was characterized throughout the modifications observed in the characteristics of PD pulses during the entire failure process. It could be verified that there is information about the deterioration of the medium contained in the characteristics of the analyzed pulses.

Key words: Partial discharge, entropy, epoxy resin, wavelet transform.

1. Introduction

A partial discharge (PD) is a localized electrical discharge, which takes place within an insulating material, caused by the presence of gaseous occlusions or impurities [1, 2]. Currently, the measurement of PD is used as a diagnostic tool [3-6]. The interpretation of its results is based on the morphology analysis that the PD pattern exhibits [1-5]. According to the shape presented, the type of failure is inferred (internal PD, superficial or corona), but nothing is known about the remnant of the useful life of the medium. This method of analysis allows characterizing the stochastic behavior of the phenomenon in a statistically way [1-5]. It is known that its occurrence inside a solid insulator (epoxy resin), causes local deteriorations of a progressive nature; this is due to two processes observed by Morshuis [7]:

- chemical degradation, due to the formation of by-products that locally modify the environment where PD manifests itself;
- physical attack, by particle bombardment.

These complex processes, although not well understood [2-4] radically modify the conditions of PD occurrence and the way they manifest as current pulses. If we also take into consideration the electronic recombination phenomena and diffusion processes [4], the phenomenological understanding of the failure process becomes even more complex.

Currently, the possibility to get high speed and high bandwidth acquisition systems, allows obtaining pulses with high temporal resolution [8]. In recent decades,

Corresponding author: Cristian Roberto Bonini, research associate, research field: partial discharge measurement in thermostable polymers.

some researchers have used waveform of current pulses (WCP) as an analysis object for classification propose of different PD configurations in epoxy resin specimens [3, 4, 9] . In the present paper, the use of WCP is used to identify different deterioration stages.

In this work, PD pulses obtained from 6 different specimens are analyzed through the whole test time until failure occurs. The Shannon entropy over the PD pulses was calculated, and its variations were analyzed. Results show that variations in standard deviations of the entropy are related with the degradation process of the specimens.

The paper is followed by the experimental development, where test specimens and lay-out are presented followed by the data acquisition and processing procedure together with the basis of Shannon entropy calculus. Then, the results are presented and analyzed and finally discussions and conclusions are presented.

2. Experimental Development

2.1 Adopted Electrode Configuration

To perform the test, a tip-plane configuration was used [10, 11]. The potential-connected electrodes were JEMCO electro-acupuncture needles of 0.2 millimeters of diameter, copper handle and a radius of curvature at its tip of 3 micrometers. To build the epoxy resin specimens, 6 specially designed aluminum matrices were used. These matrices were cured with silicone at a high temperature (200 ºC for 60 minutes). The electrodes were located at the midpoint of each matrix with respect to their sides, at a distance of 1.5 ± 0.1 millimeters measured from the lower surface of the matrix to the tip of the needle. The obtained specimen was a straight prism of 23 by 23 millimeters of base and 10 millimeters of height, see Fig. 1.

2.2 Preparation of Specimen

The proportions used to prepare the specimens were 70/30 (by weight) resin-hardener respectively, for this purpose it was used an electronic scale DENVER INSTRUMENT, model MXX-10. To obtain specimens with similar characteristics and reproducibility during tests, all specimens were built together. The dielectric resin was preheated to 25 ºC before being mixed for 5 minutes with its corresponding hardener. The increase in temperature markedly decreases the viscosity of the resin allowing to:

- obtain mixtures of uniform structure;
- get more fluidity when doing the casting;
- secure better conditions to evacuate gaseous occlusions inside the resin.

Latter, the full batch of specimens was placed in a vacuum chamber BIOMERICAN SCIENCE Model ES-300 at 720 millimeters of vacuum mercury for 90 minutes, the final curing was 24 hours at room temperature and controlled atmosphere. Then each specimen was unmolded and the lower surface was polished. Fine-grained polishing paste, less than 3 microns was used, obtaining excellent surface finishes. This allowed achieving an optimum support between the test specimen and the electrode connected to ground, avoiding local electrical field convergences that could cause the occurrence of undesired PD events.

2.3 Test Setup

The specimens were tested in the laboratory under controlled conditions in a Faraday cage. To avoid

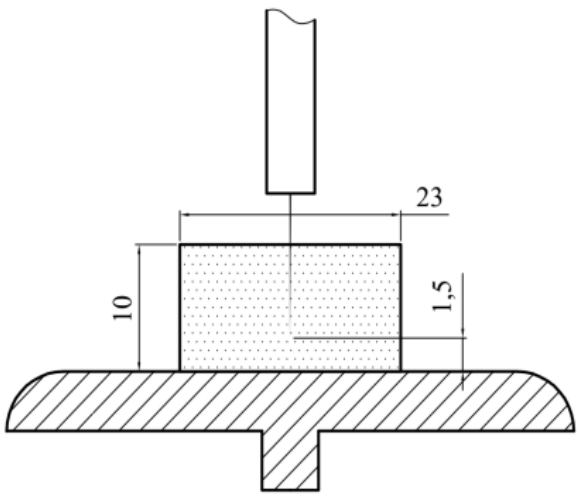

Fig. 1 Electrode configuration of the specimens.

surface discharges and/or creepage currents, they were immersed in a dielectric oil (YPF 64) bath. The adopted test voltage was 13.5 kV rms, 50 Hz, and was provided by a high voltage source model CONIMED RD-40 that fed the circuit through a current limiting protection resistor. To improve the sensitivity of the measurement system, a 150 pF and 42 kV coupling capacitor was used connected in parallel with the test specimen. In order to avoid discharges in air (corona effect) the connections between equipment and elements were made with rigid copper tubes of 12.5 millimeters of diameter (see Fig. 2). Before starting the tests, the absence of PD was verified, both in the equipment and in the used elements.

2.4 Data Acquisition

For the acquisition of the PD pulses, a commercial high frequency current transformer (HFCT) and a digital storage oscilloscope (DSO) (model Agilent DSOX2024A) with 200 MHz bandwidth connected to a Hewlett Packard 420 personal computer (PC) were used.

PD events were acquired at a sampling rate of 2 Gs/sec with a temporary window of 500 nanoseconds. Each pulse was stored in a memory segment of 1,000 length samples. Once the 250 segments, in which the DSO memory was partitioned are completed, the DSO transfers the complete record (250 pulses) to the PC and it is placed on hold mode for 60 seconds. The acquisition-waiting process is repeated cyclically from the beginning of the failure process to the test specimen perforation.

2.5 Data Processing

2.5.1 Ensemble of Records

Each record (250 pulses) acquired was concatenated with the following one, to obtain a new matrix of "*n*" pulses of 1,000 points of length (with "*n*" the total number of PD pulses acquired for a test specimen). In order to improve the efficiency of the processing algorithms, a matrix of zeros was assembled to obtain dyadic lengths of 1,024 points per pulse.

2.5.2 Denoising with Discrete Wavelet Transform (DWT)

It is known that background noise is an inherent factor in any process of signal acquisition, which is presented in an additive way to the acquired pulses [12-16]. According to Refs. [12-13] this noise can be

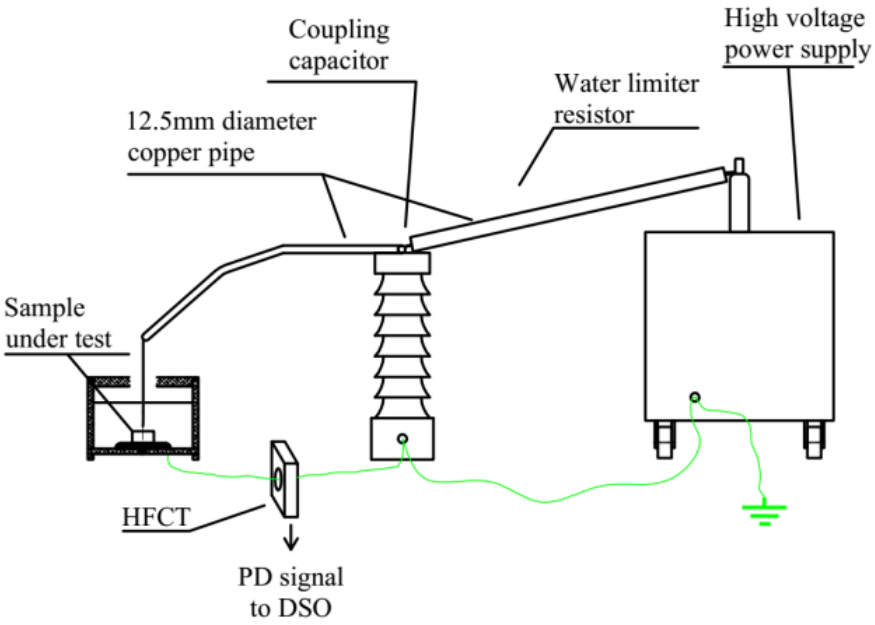

Fig. 2 Measurement scheme.

easily removed using denoising techniques deduced from the multiresolution analysis (MRA) corresponding to the DWT.

The wavelet used in the present work was a Daubechies 10 (Db10) [12, 13, 16], because of its high correlation with the structural shape of the pulse. The criterion adopted to remove the background noise was eliminating the detail coefficients d1, d2 and d3 obtained from the MRA. It could be verified that the detailed signals reconstructed from these coefficients, presented frequency components located above the HFCT upper cutoff frequency.

Then, the denoised pulses are normalized and the PD pulses matrix of each specimen is ready to be processed with the tools that are detailed in the course of this document.

2.5.3 Calculation of Entropy

Entropy is defined as a measure of disorder, a quantification of the different states in which a system can be found [17]. Actually, the information entropy introduced by Shannon [18] is used to determine the degree of randomness or disorder that a temporal sequence presents. This analysis tool is capable of extracting information and/or characterizing signals in cases where traditional methods are inefficient.

In the present work, Shannon entropy is used as an indicator, able to identify structural differences in PD pulses during the entire failure process. As was mentioned before, variations in the environment of the PD source, will influence the electron avalanche, thus the PD pulse shape is captured by the DSO. The expression that allows the calculation of the entropy is presented in Eq. (1).

$$s = -\sum_{i=1}^{n} p_i \log(p_i) \quad (1)$$

A 20-class intervals histogram to each acquired pulse was made. Each interval was divided by the length of the pulse (1,024 points), obtaining the discrete probability density curve, in which "p_i" represents the probability that some samples of the pulse coincide in the "*i*" interval. In this way, we can obtain the entropy value of each PD pulse, which will allow us to characterize them along the duration of the test. In this sense, the entropy value of each pulse along the duration of the test is represented in a reference system (see Fig. 3). From Fig. 3, we can visualize the variation of the pulse entropy and it will be analyzed in the next section.

3. Results Obtained

The results obtained on six tested specimens have yielded similar results. Different class intervals (10, 20, 30, 40 and 50) were tested and no major variations were found.

Variation of the entropy along the evolution of the failure, allowed us to identify a strong divergence of this amount respect to its average value (close to 2) as long as the failure process evolves. As Fig. 3 shows, the dispersion observed in these values increases during the entire failure process. This indicates that, along the deterioration of the specimens evolves, new pulses of different entropy values appear, increasing in this sense the dispersion of the whole entropy value, as can be seen in Fig. 4.

In order to deepen the analyses, one particular specimen (specimen No. 2) will be deeply analyzed.

3.1 Entropic Features

As was mentioned before, in the evolution of the failure process new pulses arise with entropy values that diverge from the mean value of entropy. In order to discriminate these different families of PD, the following criterion was adopted based on the calculated entropy values:

- An accumulated frequency chart (100 class intervals) was made with the entropy values obtained during the entire failure process (see Fig. 5).
- Values lower than 1% of the accumulated data were considered as pulses of low entropy (LS).
- Values greater than 99% of the accumulated data were considered as pulses of high entropy (HS).

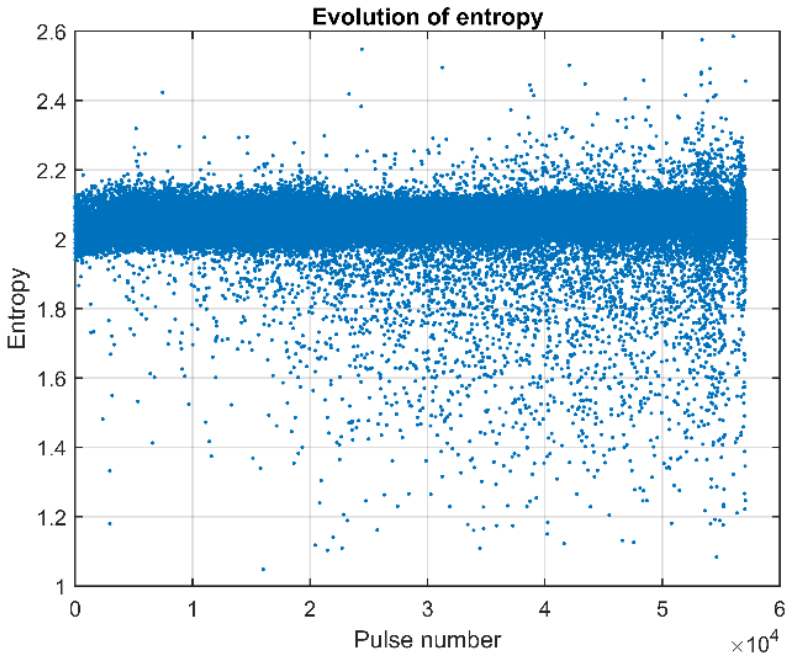

Fig. 3 Evolution of the values of entropy test specimen.

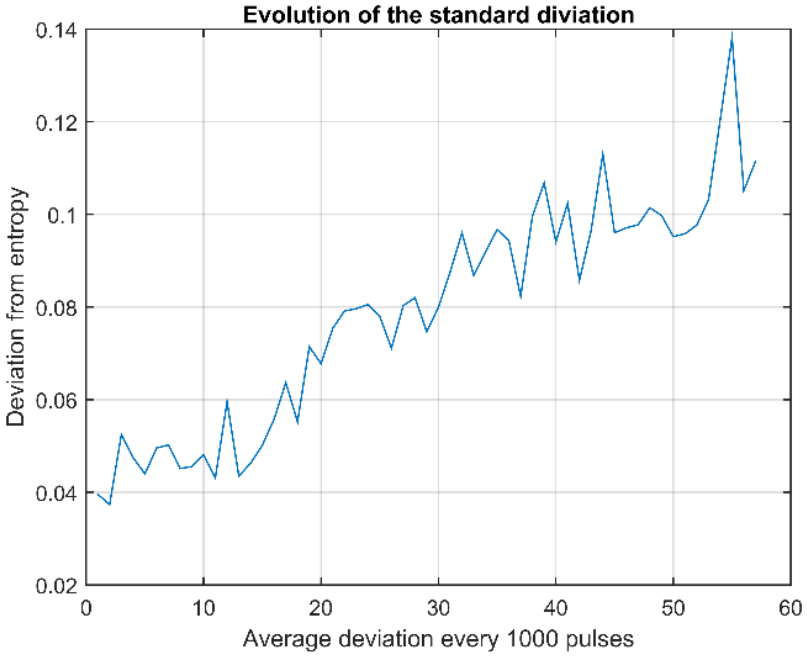

Fig. 4 Evolution of the average values of deviation of entropy.

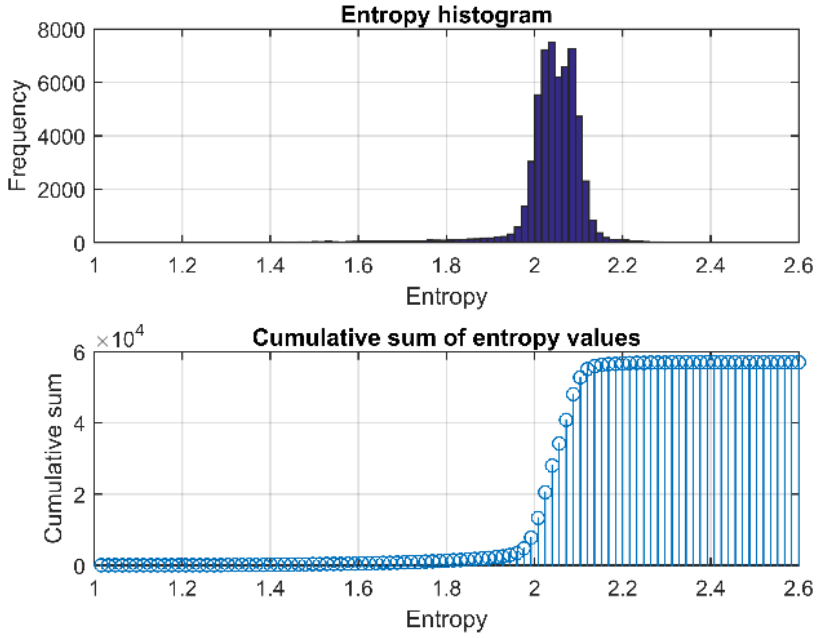

Fig. 5 Accumulative frequency of entropy for specimen No. 2.

Table 1 Entropy thresholds.

Entropy "S"	Reference	Number of pulses
S ≥ 2.17	HS	554
S > 1.64 & S < 2.17	"S" medium	55,954
S ≤ 1.64	LS	552

Table 1 shows the entropy threshold calculated values and the pulse quantities for each group corresponding to the tested specimen analyzed.

Fig. 6 shows how the divergence in the entropy values operates as a strong indicator of the deterioration process. It is observed that as the fault evolves locally deteriorating the insulating medium [10, 11, 19], different pulses with different entropic characteristics are manifested. The evolution of this deterioration has a correlation with the appearance of a greater number of pulses, whose entropy values diverge from average value (close to 2), as Fig. 6 shows.

In order to analyze and quantify how the number of PD of high and low entropy increases during the entire failure process, the analysis unit (AU) is defined as:

$$\frac{\text{number of total pulses}}{1000} = AU \qquad (2)$$

Then, an accumulated sum graph is made for high and low entropy pulses for each AU obtained.

Fig. 7 shows, as the deterioration process goes on, the number of high and low entropy phenomena increases in each AU. This increase accounts the spatial advance of the failure and the local deterioration of the environment caused by the PD occurrence. This analysis was repeated individually for each specimen, obtaining the graphs presented in Figs. 8 and 9, where it shows how this evolutionary behavior is repeated in each of the tested specimens.

3.2 Structural Characteristics

In order to deeply analyze the high and low entropy families, a spectral analysis with Fourier transform and DWT was performed to each family. In the present work, the spectral study and analysis is focusing on low and high entropy pulses, because they are the ones that show the deterioration process by diverging from the average entropy pulses as the failure evolves.

First, for each specimen, HE and LE pulses were separated with the criteria presented in Section 3.1, then the PD pulses corresponding to each family were mathematically processed in order to identify their

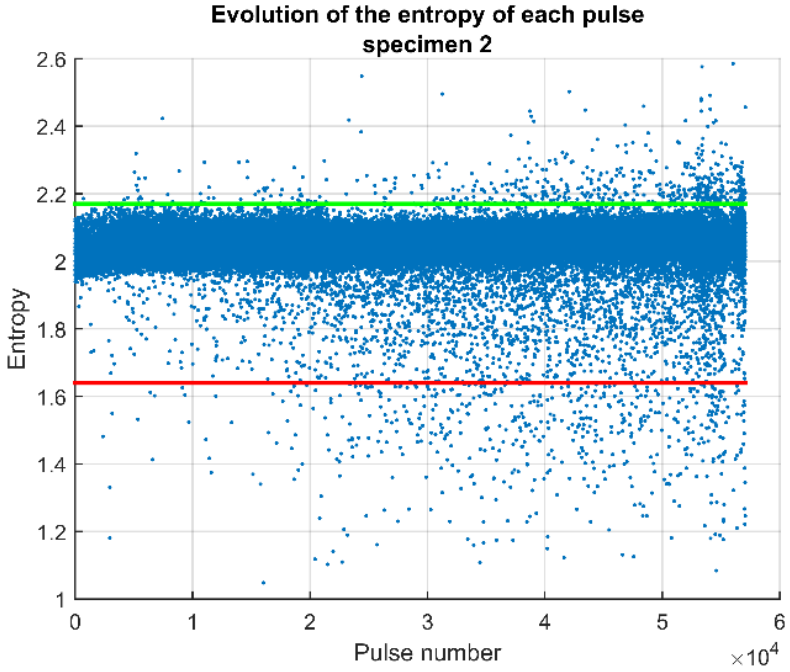

Fig. 6 Evolution of values of entropy and its thresholds, specimen No. 2.

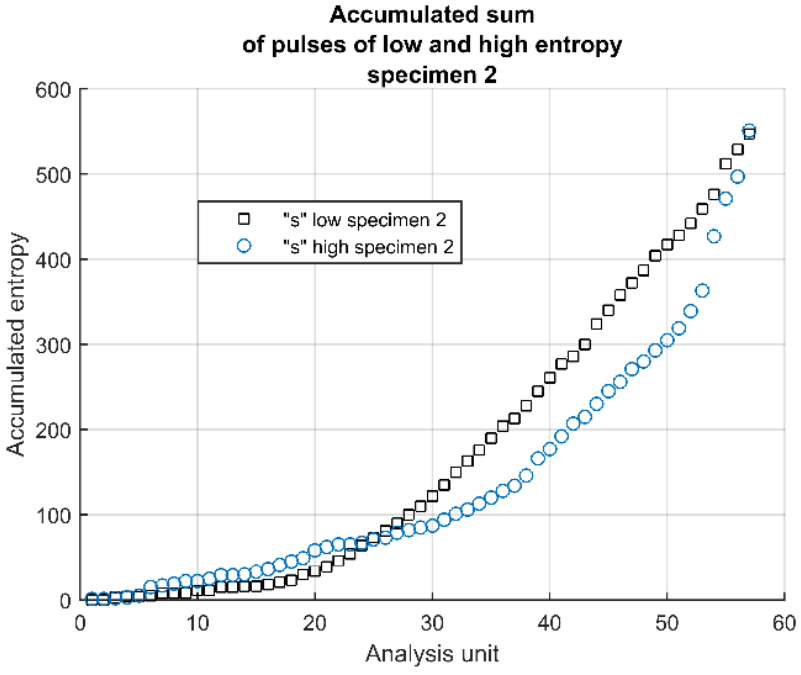

Fig. 7 Accumulated frequency of pulses of low and high entropy, specimen No. 2.

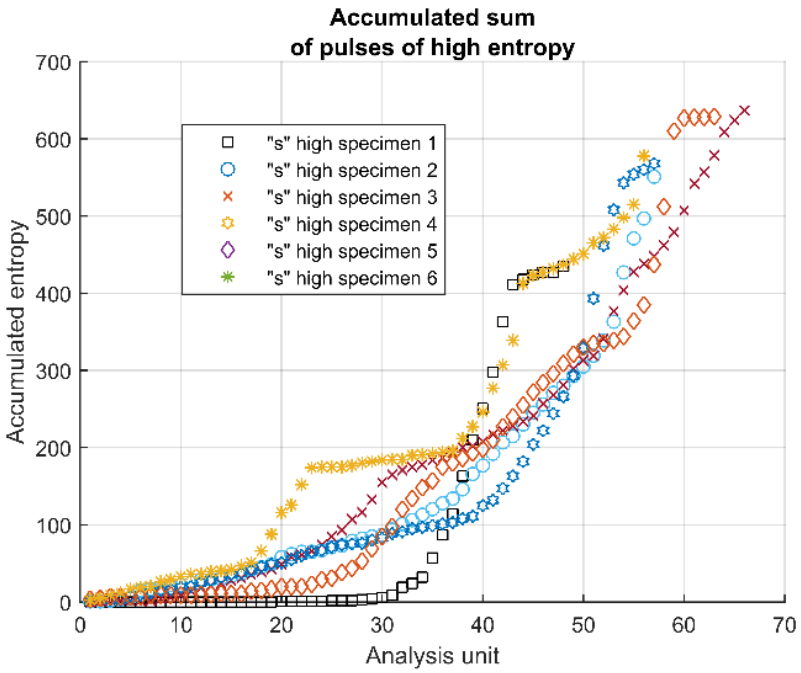

Fig. 8 Accumulated frequency of pulses of high entropy, corresponding to the 6 tested specimens.

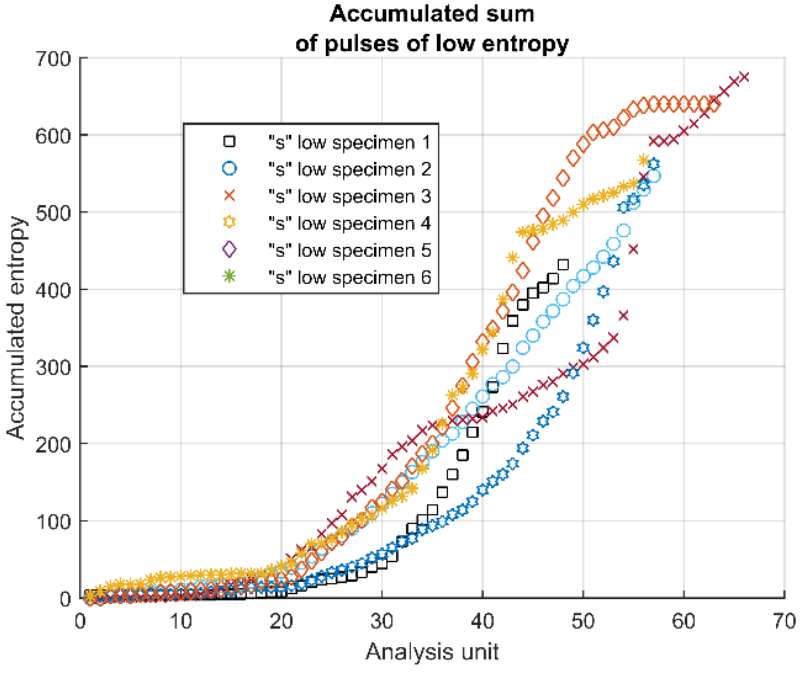

Fig. 9 Accumulated frequency of pulses of low entropy, corresponding to the 6 tested specimens.

underlying characteristics. The differences observed in the structural shape of the pulses were characterized using the fast Fourier transform (FFT), which allowed the identification of essential differences in their spectral content; lastly, pulses were analyzed with DWT to quantize the energy distribution in different frequency bands.

3.2.1 Spectral Analysis

In Fig. 10, the morphological and spectral differences of pulses corresponding to different

families can be observed. Some of the relevant characteristics showed are listed below:

(1) Low Entropy Pulses

- Low frequency components.
- Greater bandwidth.
- In its spectrum a predominant frequency is not observed.
- The energy is distributed more evenly than in the high entropy pulses.

(2) High Entropy Pulses

- Spectrum and energy bounded in a reduced bandwidth.
- Main component defined 24 MHz.

3.2.2 Discrete Wavelet Transform

To compare energy distribution in the frequency domain, the DWT was employed. The DWT analysis allows the decomposition of a signal in different frequency bands by the filter bank algorithm. In the present work, the detail coefficients of decomposition level 4, 5 and 6 (d4, d5 and d6) are used. Higher decomposition levels have not been taken into account because they contain less than 10% of the total energy of the pulse. Then, the energy of each detail coefficient was obtained by Eq. (3) [20], and the mean and deviation for each family and specimen was calculated.

$$E = \sum_{n} |\boldsymbol{x}[\boldsymbol{n}]|^2 \tag{3}$$

From the analysis carried out, it was found that the energy at the different levels of detail is differently distributed between pulses of low and high entropy. Figs. 11 and 12 show average energy and deviation values of each detail level for each tested specimen.

For high entropy pulses, the main energy is located at d5 (see Fig. 12) in concordance with a main component mentioned in Fig. 10. In the same sense, for the low entropy family, the energy is more evenly distributed in the three selected bands.

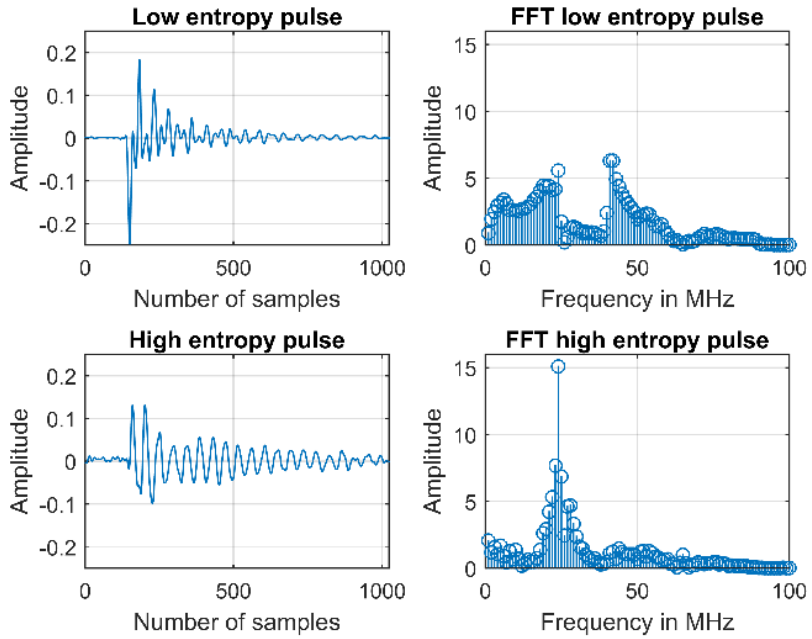

Fig. 10 Pulses of low and high entropy with its corresponding spectra.

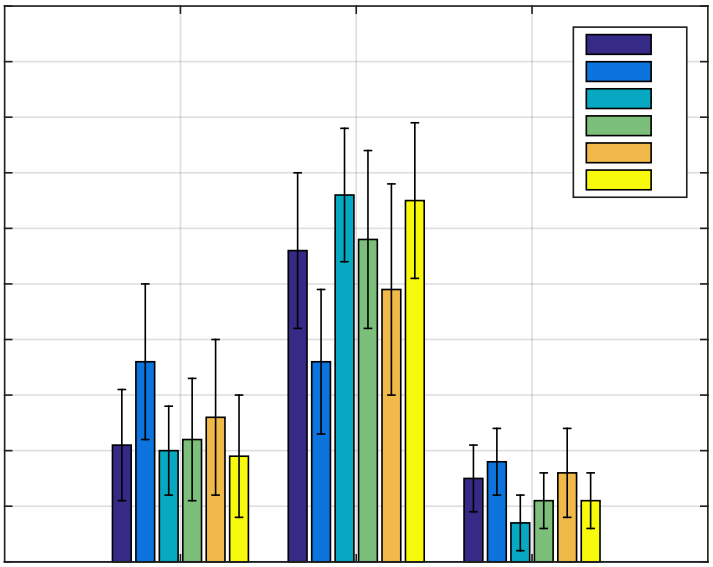

Fig. 11 Energy of the details d4, d5 and d6 corresponding to low entropy pulses of the 6 specimens.

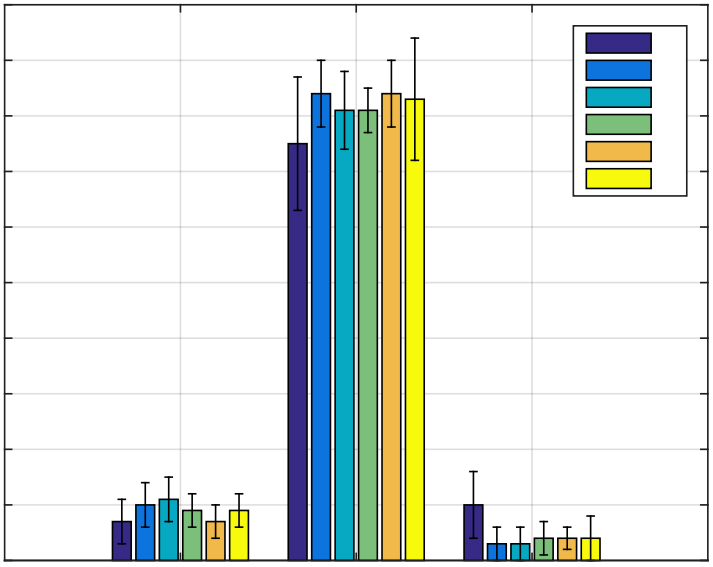

Fig. 12 Energy of the details d4, d5 and d6 corresponding to high entropy pulses of the 6 specimens.

4. Discussion and Conclusions

In this work, the deterioration of 6 epoxy resin specimens was characterized by means of the entropy of PD pulses recorded along the test procedure. It was found that the entropy was able to detect modifications in the observed PD pulses during the entire failure process. The results obtained have been consistent during all the tested specimens.

The tests and analyses performed on the acquired pulses, allowed the detection of valuable information which indicates that a deterioration process is active. As was shown in Figs. 3 and 4, changes in the entropy dispersion of the acquired pulses allowed identifying this process.

Thereby, it was observed that as the fault evolves, new pulses of different entropy value arise, which increase the total entropy dispersion. In this sense, the number of PD pulses of low and high entropy will increase as long as the deterioration evolves, as was emphasized with the AU presented in Figs. 8 and 9. The quantitative differences observed in these values, allowed the identification of different families (pulses of high and low entropy) with different spectral characteristics.

The spectral analysis (FFT) allowed observing important differences in the frequency domain of the families; identifying different bandwidth and different spectral distribution. To analyze this energy distribution, time-scale analysis (DWT) was employed and low and high entropy pulses were characterized in terms of energy distribution in the three main frequency bands. It could be verified that the low entropy pulses present approximately 90% of their energy distributed between the detail levels d4, d5 and d6; while the high entropy pulses distribute this percentage between the detail levels d4 and d5. In this same sense, the high entropy pulses concentrate the greatest amount of energy in the detail level 5.

Further studies should be dedicated to research how to determinate the proper boundaries for high and low entropy pulses definition. In addition, in order to have a prior-to-failure indicator, the maximum number of pulses of high/low entropy as well as the deviation in the whole entropy value prior to failure should be deeply analyzed. To fulfill these fundamentals points, more tests and studies are being carried out.

References

[1] Schurch, R., Orellana, L., Donoso, P., Ardila-Rey, J., and Montana, J. 2017. “Pulse Waveform, Phase-Resolved and Pulse Sequence Analysis of Partial Discharges during Electrical Tree Growth in Epoxy Resin.” Presented at the 20th International Symposium on High Voltage Engineering, Buenos Aires, Argentina.

[2] Boggs, S., and Densley, J. 2000. “Fundamentals of Partial Discharge in the Context of Field Cable Testing.” *IEEE Electr. Insul. Mag.* 16 (5): 13-8.

[3] Okubo, H., Hayakawa, N., and Matsushita, A. 2002. “The Relationship between Partial Discharge Current Pulse Waveforms and Physical Mechanisms.” *IEEE Electr. Insul. Mag.* 18 (3).

[4] Okubo, H., and Hayakawa, N. 2005. “A Novel Technique for Partial Discharge and Breakdown Investigation Based on Current Pulse Waveform Analysis.” *IEEE Electr. Insul. Mag.* 12 (4): 736-44.

[5] Montanari, G. C., and Cavallini, A. 2013. “Partial Discharge Diagnostics: From Apparatus Monitoring to Smart Grid Assessment.” *IEEE Electr. Insul. Mag.* 29 (3): 8-17.

[6] Wu, M., Cao, H., Cao, J., Nguyen, H., Gomez, J. B., and Krishnaswamy, S. P. 2015. “An Overview of State of the Art Partial Discharge Analysis Techniques for Condition Monitoring.” *IEEE Electrical Insulation Magazine* 31 (6): 22-35.

[7] Morshuis, P. H. F. 2005. “Degradation of Solid Dielectrics Due to Internal Partial Discharge: Some Thoughts on Progress Made and Where to Go Now.” *IEEE Transactions on Dielectrics and Electrical Insulation* 12 (5): 905-13.

[8] Maillot, M. U., and Pessana, F. M. 2018. “A New Feature Space Formation Based on DWT Coefficient Variance for Partial Discharge Classification.” *Journal of Electrical Engineering* 6 (1): 18-27.

[9] Sahoo, N. C., Salama, M. M. A., and Bartnikas, R. 2005. “Trends in Partial Discharge Pattern Classification: A Survey.” *IEEE Transactions on Dielectrics and Electrical Insulation* 12 (2).

[10] Schurch, R., Rowland, S. M., and Bradley, R. S. 2015. “Partial Discharge Energy and Electrical Tree Volume

Degraded in Epoxy Resin." Presented at IEEE Conference on Electrical Insulation and Dielectric Phenomena, 820-3.

[11] Rowland, S. M., Schurch, R., Pattouras, M., and Li, Q. 2015. "Application of FEA to Image-Based Models of Electrical Trees with Uniform Conductivity." *IEEE Trans. Dielectr. Electr. Insul.* 22: 1537-46.

[12] Soman, K. P., Ramachandran, K. I., and Resmi, N. G. 2010. *Insight into Wavelets from Theory to Practice*. 3rd ed., PHI Learning.

[13] Mallat, S. 1999. *A Wavelet Tour of Signal Processing*. 2nd ed., San Diego, California: Academic Press.

[14] Sirne, R. O., and D'attellis, C. E. 2004. *Introducción a Onditas, con Aplicación a la Caracterización Frecuencial de ECG*. Centro de Procesamiento de Señales e Imágenes.

[15] D'attellis, C., Anaya, M. T., Cavallaro, M. I., and Villaverde, F. F. 2012. *Introducción a las Onditas*. Segunda edición, Nueva Librería.

[16] Wevelet Toolbox. 2015. "Analyze and Synthesize Signals and Images Using Wavelets." https://la.mathworks.com/products/wavelet.html.

[17] Jaynes, E. T. 2003. *Probability Theory, the Logic Science*. Cambridge University Press.

[18] Shannon, C. E. 1948. *A Mathematical Theory of Communication*. Reprinted with Corrections from *the Bell System Technical Journal* 27: 379-423, 623-56.

[19] Schurch, R., Rowland, S. M., Bradley, R. S., and Withers, P. J. 2014. "Imaging and Analysis Techniques for Electrical Trees Using X-ray Computed Tomography." *IEEE Trans. Dielectr. Electr. Insul.* 21 (1): 53-63.

[20] Craiem, D., and Armentano, R. L. 2011. *Análisis de Sistemas Lineales*. Centro de Estudiantes de Ingeniería Tecnológica—CEIT.